Observations of the Directional Characteristics of Sea Waves

J. H. Simpson

Summary

Simultaneous records of orbital velocity and pressure disturbance in wind generated waves have been analysed by power spectral methods, to obtain the first five angular harmonics of the directional spectrum. The observations were made at a coastal site, offshore from a gently sloping beach, where the bottom topography was sufficiently simple to permit corrections for the effects of refraction. The orbital velocities were measured by an electromagnetic flowmeter and the pressure disturbance by an N.I.O. pressure recorder. A capacitance probe was also available for recording the surface elevation. A computer program has been developed which computes the auto and cross-spectra of the pressure and velocity components, the angular harmonics and a smoothed estimate of the directional spectrum directly from data which were recorded digitally on punched paper tape.

Estimates of the mean direction and the width of the directional spectrum and its skewness, have been obtained for a wide range of frequencies and related to wind conditions in the generating area. After correction for refraction, the mean direction of the waves was found to correspond well to the mean wind direction. For waves generated by a reasonably constant wind field, the spectrum width exhibits a general tendency to increase with frequency. At low frequencies the spectrum width corrected for refraction is not inconsistent with the resonance angle given by Phillips' theory, while at frequencies just above the transition frequency defined by the combined Miles–Phillips theory, the spectrum is appreciably narrower than the resonance angle. The smoothed directional spectrum estimate based on five harmonics gives no indication of bimodality in the spectrum. A method of obtaining improved angular resolution using an array of three flowmeters to obtain four additional harmonics was only partially successful on account of turbulent interference generated by the pier structure to which the sea units were attached.

The surface power spectrum was found to fit the equilibrium power law at high frequencies under saturation conditions. A spectrum obtained under conditions very similar to those in the SWOP project has been compared with the SWOP spectrum. Marked differences between the two suggest that bottom friction is a major influence on waves in coastal waters.

The attenuation of the waves in depth was determined from the ratios of the surface elevation and pressure spectra. No significant departure

from the attenuation law based on linear theory was found in any part of the spectrum where the coherency between the surface elevation and pressure was high.

The ratio of the velocity and pressure spectra was also found to be consistent with linear theory, thus confirming the relation between wavelength and frequency in water of finite depth.

The amount of wave energy reflected from the shore proved to be negligible. The amplitude reflection coefficient, which was deduced from the relative phase of the pressure and velocity, is of order 0·05.

Notation

$\mathbf{x} = (x, y)$	horizontal space co-ordinate;
z	vertical co-ordinate measured upwards from the mean level;
t	time co-ordinate;
θ	horizontal directional co-ordinate;
$\eta(x, y, t)$	surface elevation from the mean level;
$\phi(x, y, z, t)$	velocity potential;
h	mean depth;
c	phase velocity;
$\mathbf{k}$	vector wave number;
$\sigma = 2\pi f$	angular frequency;
ε	phase angle;
u, v	horizontal velocity components;
p	pressure variation from the mean;
$H(z)$	attenuation factor;
$c(pp)$	auto spectra;
$c(up), q(up)$	co- and quadrature spectra;
A_n, B_n	angular harmonics;
$F(\sigma, \theta)$	directional spectrum;
$\gamma(\sigma)$	coherency of two time series;
$\Delta\phi(\sigma)$	relative phase of two time series;
$\bar{\theta}$	mean direction of the waves.

1. Introduction

The use of an electromagnetic flowmeter and pressure recorder to determine the first five harmonics of the directional spectrum of sea waves has been described in a previous paper (Bowden & White 1966). These earlier observations were made at a site in the Mersey estuary where wave conditions were greatly influenced by refraction in shallow water and the strong tidal currents in the estuary. It was not therefore possible to relate the results to conditions prevailing in the generating area. The observations reported here were made at a more exposed site where conditions were representative of the open sea, so that the results may be compared with the recent theories of wave generation (Phillips (1957, 1966), Miles (1957, 1967)).

The main limitation of the single flowmeter method is the rather severe smoothing it imposes on the directional spectrum. In an effort to improve the directional resolution an array of three flowmeters has been used to measure the horizontal derivatives of the velocity, from which a further four harmonics of the directional spectrum may be determined.

In the previous observations a bottom mounted pressure recorder was used in conjunction with a flowmeter located 2–3 m above the bottom. Since the results suggested that the attenuation of pressure and velocity did not always conform closely to the attenuation laws given by infinitesimal wave theory, it was decided to fix the flowmeter and pressure transducer at the same height and to investigate the attenuation effect independently by using a surface level recorder. To reduce the amount of time and labour involved in processing the observations, the data were recorded directly on punched tape using a digital logging device and a computer programme developed which would perform the complete analysis from raw data to directional spectrum in one operation.

2. Theory

2.1 *The directional spectrum*

As a model of the sea surface we take a linear combination of sinusoids of the form (Cartwright 1962)

$$\eta = \sum_{n=1}^{\infty} a_n \sin (k_n \cos \theta_n \, x + k_n \sin \theta_n \, y - \sigma_n \, t + \varepsilon_n), \qquad (2.1)$$

where the k_n and ε_n are densely distributed over $(0 < k_n < \infty; \; 0 \leqslant \theta \leqslant 2\pi)$. The phases ε_n are treated as random variables so that equation (2.1) represents an ensemble of possible sea states.

The velocity potential corresponding to a single sinusoidal component is given by solution of the hydrodynamic equations under linearising assumptions (Lamb 1932, p. 369) as

$$\phi = \frac{g a_n}{\sigma_n} H_n(z) \quad (\cos \mathbf{k}_n \, \mathbf{x} - \sigma_n \, t + \varepsilon_n)$$

$$H_n(z) = \frac{\cosh k_n (z+h)}{\cosh kh} \; ; \quad \mathbf{k}_n = (k_n \cos \theta, \; k_n \sin \theta),$$

where the wave number k_n and the angular frequency σ_n are related by

$$\sigma_n^2 = g k_n \tanh k_n \, h.$$

The combined velocity potential corresponding to equation (2.1) may thus be written as

$$\phi = \sum_{n=1}^{\infty} \frac{g a_n}{\sigma_n} H_n \cos \chi_n : \chi_n = \mathbf{k}_n \cdot \mathbf{x} - \sigma_n \, t + \varepsilon_n,$$

for which the horizontal velocity components are found to be

$$u = -\frac{\partial \phi}{\partial x} = \sum_{n=1}^{\infty} \frac{g H_n}{\sigma_n} a_n k_n \cos \theta_n \sin \chi_n$$

$$v = -\frac{\partial \phi}{\partial y} = \sum_{n=1}^{\infty} \frac{g H_n}{\sigma_n} a_n k_n \sin \theta_n \sin \chi_n$$

similarly the pressure variation from the mean is just

$$p = \frac{1}{g} \frac{\partial \phi}{\partial t} = \sum_{n=1}^{\infty} a_n H_n \sin \chi_n$$

if p is measured in centimetres of water or similar units.

The ensemble of surfaces represented by equation (2.1) are related through the directional spectrum which is defined as:

$$F(\sigma, \theta) = \frac{1}{\Delta\sigma \, \Delta\theta} \sum_{\Delta\theta} \sum_{\Delta\sigma} \tfrac{1}{2} a_n^2.$$

We shall also find it convenient to use the modified directional spectrum

$$F'(\sigma, \theta) = F(\sigma, \theta) H^2(\sigma) = \frac{1}{\Delta\sigma \, \Delta\theta} \sum_{\Delta\theta} \sum_{\Delta\sigma} \tfrac{1}{2} a_n^2 H_n^2$$

and to express $F'(\sigma, \theta)$ as a Fourier series in terms of the angular harmonics A_n and B_n:

$$F'(\sigma, \theta) = \tfrac{1}{2}A_0 + \sum_1^m \{A_n \cos n\theta + B_n \sin n\theta\}$$

in which

$$A_n + iB_n = \frac{1}{\pi} \int_0^{2\pi} e^{in\theta} F'(\sigma, \theta) \, d\theta.$$

We have available the three components p, u and v, from which we may deduce the first few A_n and B_n. As a first step we consider the auto and cross-spectra of p, u and v which may be obtained from the wave observations by the usual digital processes (Blackman & Tukey 1958).

In terms of the auto and cross-spectra the first five angular harmonics are just

$$A_0 = \frac{c(pp)}{\pi}$$

$$A_1 = \frac{c(up)}{\pi} \frac{\sigma}{gk}; \quad B_1 = \frac{c(vp)}{\pi} \frac{\sigma}{gk}$$

$$A_2 = \frac{c(uu) - c(vv)}{\pi} \left(\frac{\sigma}{gk}\right)^2; \quad B_2 = \frac{2c(uv)}{\pi} \left(\frac{\sigma}{gk}\right)^2.$$

From these angular harmonics a smoothed estimate of the modified directional spectrum may be obtained.

$$F'(\sigma, \theta) = \tfrac{1}{2}A_0 + w_1(A_1 \sin\theta + B_1 \sin\theta) + w_2(A_2 \cos 2\theta + B_2 \sin 2\theta)$$

$$= \int_0^{2\pi} F'(\sigma, \theta') \, W(\theta - \theta') \, d\theta',$$

where the choice $w_1 = \tfrac{2}{3}$; $w_2 = \tfrac{1}{6}$ gives a suitable non-negative form of the smoothing function $W(\theta - \theta')$.

As a measure of the mean direction of the waves we have $\bar\theta = \tan^{-1} B_1/A_1$ and for a narrow spectrum the moments about this mean direction are (Cartwright 1961)

$$m_2 = \overline{(\theta - \bar\theta)^2} = 2 \left(1 - \frac{C_1}{A_0}\right); \quad C_1^2 = A_1^2 + B_1^2,$$

$$m_3 = \overline{(\theta - \bar\theta)^3} = 2\bar\theta - \tan^{-1} B_2/A_2.$$
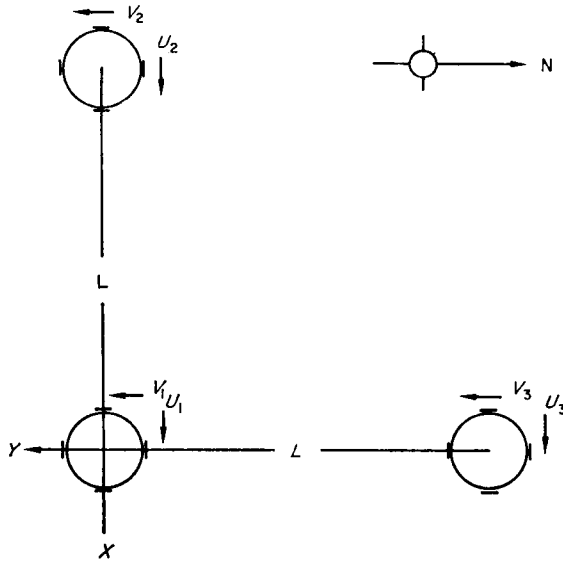
FIG. 1. Triangular array of flowmeters.

An alternative width parameter equivalent to m_2 may be defined (Longuet-Higgins, Cartwright & Smith (1961)) as

$$\sin^2 \frac{\psi}{2} = \tfrac{1}{2}\left(1 - \frac{C_1}{A_0}\right).$$

2.2 The velocity derivatives

Improved directional resolution may, in principle, be obtained by measuring the quantities $\partial u/\partial x$, $\partial u/\partial y$, $\partial v/\partial x$, $\partial v/\partial y$. These derivatives of the horizontal velocity components can be obtained from a triangular array of flowmeters. For the array shown in Fig. 1 we have for the three independent quantities ($\partial u/\partial y = \partial v/\partial x$ for irrotational flow).

$$u_x = \frac{\partial u}{\partial x} \doteq \frac{u_1 - u_2}{L};$$

$$u_y = \frac{\partial u}{\partial y} \doteq \frac{u_1 - u_3}{L}$$

$$v_y = \frac{\partial v}{\partial y} \doteq \frac{v_1 - v_3}{L}.$$

On account of the finite spacing of the flowmeters these estimates of the derivatives are subject to an error of order

$$e \doteq \tfrac{1}{2}L \left|\frac{\partial^2 u}{\partial x^2}\right| \bigg/ \left|\frac{\partial u}{\partial x}\right| = \frac{\pi L}{\lambda}.$$

To minimize this error we require the array spacing $L \ll \lambda$. On the other hand the signal to noise ratio of the finite differences $u_1 - u_2$ etc. must be maintained at a reasonable level. The difference $u_1 - u_2$ is of order $(2\pi L/\lambda)\,|u|$ and the flowmeter noise is roughly $1\,\mathrm{cm\,s^{-1}}$. For the range of λ anticipated a choice of $L = 1\mathrm{m}$ is a reasonable compromise.

The derivatives are of order $k\,|u|$ and are therefore richer at high frequencies than the velocity and pressure components. In spite of this, the derivative spectra should fall off rapidly at high frequencies on account of the attenuation with depth.

To determine the harmonics of order 3 and 4 we form the auto and cross-spectra of the derivatives and the quantities p, u and v. The spectra are related to the angular harmonics by the identities

$$\pi A_3 = \alpha c(up) - \frac{4\alpha^2}{k} q(uv_y); \quad \pi B_3 = \frac{4\alpha^2}{k} q(vu_x) - \alpha c(vp);$$

$$\pi A_4 = c(pp) - \frac{8\alpha^2}{k^2}(u_x v_y); \quad \pi B_4 = 4\alpha^2 c(uv) - \frac{8\alpha^2}{k^2} c(u_y v_y);$$

$$\alpha = \frac{\sigma}{gk}.$$

Not all the possible spectra are used in these relations. The rest are zero or equivalent to those already used. Power spectra of derivatives have been avoided, as have spectra like $c(u_x u_y)$ in which a single velocity component is involved in both time series.

The power spectra should be related by the identity

$$\delta^2 = \frac{k^2}{\alpha^2} = \big(c(u_x u_x) + 2c(u_y u_y) + c(v_y v_y)\big)/c(pp)$$

which serves as a check on the noise level.

The improved estimate of the directional spectrum including the higher harmonics is now

$$F_4(\sigma, \theta) = \tfrac{1}{2}A_0 + \sum_1^4 w_n(A_n \cos n\theta + B_n \sin n\theta).$$

A suitable choice of the w_n given by Cartwright & Smith (1964) is $w_1 = 0 \cdot 8889$, $w_2 = 0 \cdot 6222$, $w_3 = 0 \cdot 3394$, $w_4 = 0 \cdot 1414$. This yields a non-negative smoothing function in r.m.s. width of 29° which is about half of that obtained with a single flowmeter.

3. Experimental arrangements

3.1 *The recording site*

The interpretation of wave records taken near the coast is complicated by refraction and reflection of the incident waves. Refraction effects can be estimated only if the bottom contours are reasonably regular, while reflection can be sensibly eliminated by observing the waves off-shore of a gently sloping beach on which the wave energy will be dissipated.

A survey of possible sites along the Lancashire and North Wales coasts indicated that the most attractive section of beach from the point of view of slope and regularity was at Blackpool. This location was also favoured by its exposure to the prevailing south-west and westerly winds blowing over fetches up to 130 miles (see Fig. 2). An approach was made, therefore, to the management of two of the Blackpool piers about the possibility of installing wave recording apparatus. Both generously agreed to co-operate but the South Pier was finally chosen on account of the great length of cable required to reach the end of the jetty on the North Pier.

Regular wind observations are taken about a mile from the coast at Blackpool
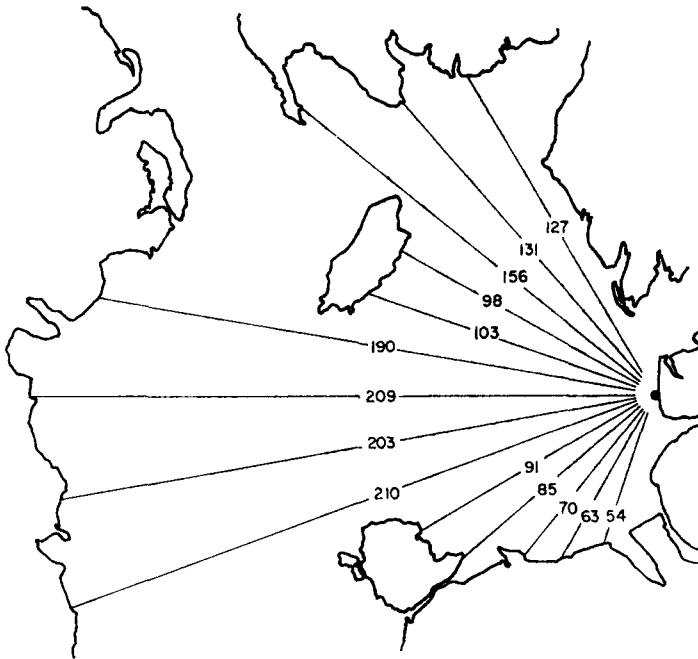
FIG. 2. Fetch in kilometres.

airport and these together with data from Valley and Ronaldsway provide adequate coverage of the relevant areas.

The South Pier is about 400 yards long and projects in a direction slightly south of west from the promenade. On high water springs there is a depth of roughly 6 m at the end of the pier. The beach level at the end of the pier is about 3·5 m above the level of the low water springs, so the base of the pier can be reached for two hours on either side of low water.

The bottom topography in the vicinity of the recording site is shown in Fig. 3. The shoreline is essentially straight from the Ribble estuary in the south to Fleetwood in the north. The bottom contours are also reasonably straight and parallel to the shoreline except for Shells Flat which will only effect waves arriving from directions between north and north-west.

The end of the pier is supported by a row of timbers approximately 30 cm square and about 7 m in height. The spacing between them is just under two metres. A scaffolding structure was attached to these timbers by means of four mild steel brackets.

The three flowmeter heads were clamped to the structure at the vertices of a right-angled triangle (side length 1 m) about 2·5 m above the bottom so that the depth of water above them was roughly 3·5 m at high water springs.

The pressure unit was fixed between two of the flowmeters with its sensing plate at the same level as the flowmeter electrodes. It was secured to the scaffolding by a pair of clamps bolted to the main casting in place of the usual base plate. The capacitance wire was fixed vertically above the other units.

The hut, an 8 ft × 6 ft reinforced garden shed, housed the electronics for the various wave recorders along with the digital logging system. A mains supply was provided by the pier authorities who also gave valuable assistance during the installation of the sea units and the cables.
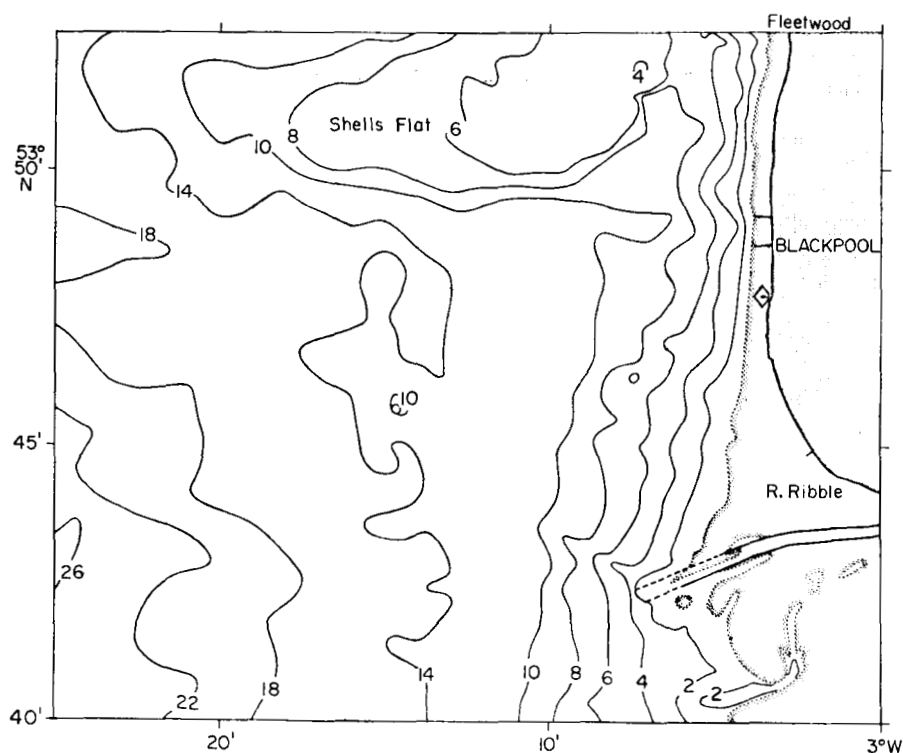
J. H. Simpson

FIG. 3. Bottom topography. Depth in metres.

3.2 Wave recorders

(a) The electromagnetic flowmeter is essentially the same as that described by Howe (1960) and Bowden & Fairbairn (1952) except for the following modifications.

1. The first stage amplifier valve EF3FA was replaced by the less microphonic EF86.

2. An anti-drift filter with RC = 8 s (matching that of the pressure recorder) was inserted between the detector and output stages.

3. The d.c. output stage was previously a differential amplifier with output floating at about 250 V relation to earth. Since a large common mode voltage is undesirable for input to the digital logging system, a differential cathode follower has been substituted for the amplifier. The output is now at a potential of 35 V relative to earth. The loss of d.c. gain reduced the overall sensitivity to approximately 130 mV cm^{-1} s^{-1}, but this is of no consequence since the digital voltmeter can still adequately resolve the signal down to the noise level.

The frequency response of the amplifiers is flat between 1 c/s and 1/20 c/s where the effect of the anti-drift filter becomes appreciable.

The three flowmeter field coils were connected in series to the 120 V supply from the balance unit. This 50 c/s voltage is derived from a mains auto transformer which replaces the 80 V isolating transformer used previously when two heads only were employed.

(b) A slightly modified version of the capacitance wire recorder described by Tucker & Charnock (1954) was built for use at Blackpool. The measuring head consists of an insulated wire stretched vertically through the water surface. A capacity exists between the metallic conductor and the surrounding water with the insulation

acting as the dielectric medium. This capacity is incorporated in the tank circuit of a tuned oscillator so that changes in capacity caused by changes in water level modulate the frequency of the oscillator. The resulting F.M. signal is fed to a discriminator which gives an output voltage proportional to frequency and hence to the water level. This may be amplified by a d.c. stage, or as in the present case, fed, via an anti-drift filter, to a cathode follower output.

The sensing wire should have a suitable capacitance per unit length and it should be sufficiently rugged to withstand heavy wave action for long periods. It is also important that the dielectric properties of the insulation are not affected by prolonged immersion in water. The wire chosen in this case was a heavy duty PVC covered wire with $\sigma = 2 \cdot 5 \, \text{pf/cm}$.

(c) A full account of the N.I.O. frequency modulated pressure recorder is given in Harris & Tucker (1963).

The pressure acts on a diaphragm whose movement varies the gap of a parallel plate capacitor which is the tuning capacitor of an LC oscillator. The resulting F.M. signal is amplified before being transmitted up the cable to the electronics unit. The signal from the sea unit passes through a broadly tuned amplifier stage before being modulated by a fixed frequency signal derived from a quartz oscillator. The difference frequency is selected by means of a low pass filter and fed to a diode pump frequency meter which gives a d.c. output proportional to the frequency fluctuation and hence to the pressure change. The frequency meter output passes to a d.c. amplifier via a high pass filter when used as a wave recorder and via a low pass filter when used as a tide gauge.

The oscillator in the sea unit has a temperature coefficient of 1 part in 10^4 °C. This is the equivalent to a change in water level of $3 \, \text{cm} \, °\text{C}^{-1}$ which is of no consequence when measuring waves. It may however have an appreciable effect if the instrument is used as a tide gauge, when a correction is also necessary for changes in atmospheric pressure.

(d) The outputs from the wave recorders were converted to digital form and punched onto paper tape by a data logging system made by Digital Measurements Ltd. Scanning speeds up to 10 channels s^{-1} were available on the system and a capacitative store facility was added which enabled a number of channels to be logged simultaneously.

3.3 The wave records

The following three types of wave record were taken:

3.3.1 *PUV records.* For the study of the directional properties of the wave motions, the two horizontal velocity components were recorded together with the pressure disturbance at the same depth. The scanning rate was four channels per second making $\Delta \tau = \frac{3}{4} \, \text{s}$ for each channel. Over 40 such records, mostly of 10 min duration, were taken in a wide variety of synoptic situations. After analysis by the directional spectrum programme, they yielded the estimates of the directional spectrum and its parameters discussed in Section 5.

3.3.2 *SP records.* In order to investigate the relation between the observed modified directional spectra and the corresponding surface spectra, simultaneous records were taken of the surface elevation and the pressure at mid-depth. Using the four channels per second scanning rate we have $\Delta \tau = \frac{1}{2} \, \text{s}$ for each channel, which is adequate to avoid aliasing of the surface elevation. Over 20 10-min records of this type were obtained, making possible a comparison of the surface elevation and pressure spectra over a wide range of frequency and amplitude.

3.3.3 *Derivative records*. In an attempt to measure the velocity derivatives and hence the higher harmonics of the directional spectrum, a number of records were also taken of the output from three flowmeters (six velocity components) together with the pressure and surface elevations. For these records the maximum scanning rate of 10 channels s^{-1} was necessary. In all, ten channels were scanned making $\Delta\tau = 1$ s for each channel. In view of the severe attenuation of the high frequency velocity components, aliasing should not be a problem with this value of $\Delta\tau$, providing that turbulence and other forms of noise do not contribute significantly to this part of the spectrum. The surface elevation was connected to two channels in the scanning sequence so that it was recorded at $\frac{1}{2}$ s intervals. The flowmeter outputs and the pressure were all recorded simultaneously by using the capacitative store.

4. The power spectra and relations between them

4.1 *Surface elevation spectrum*

Estimates of the surface elevation power spectrum were obtained from the SP records for the frequency range 0·05 c/s to 1·0 c/s. The general form of the spectrum can be seen from the selection of spectra shown in Fig. 4. The estimates have a stability corresponding to 40 degrees of freedom and are spaced at intervals of 0·0167 c/s.

Fig. 4(a) and (b) have been plotted in log–log form to permit comparison with the equilibrium range spectrum (Phillips 1958).

$$c(ss) = bg^2 \sigma^{-5}.$$

The straight line represents this spectrum for $b = 1·48 \times 10^{-2}$ deduced from Burling's (1955) data. Within the confidence limits of the analysis there is a good agreement with the observations over the high frequency part of the spectrum. At the very highest frequencies the observed points lie above the line on account of the instrument noise level.

At lower frequencies the spectra exhibit the usual sharp drop in energy to a background level which is generally higher than that found at high frequencies. The fact that the coherency between the surface elevation and the pressure is generally significant, and frequently quite high in this region of the spectrum, indicates that the background level is not due to noise originating in the capacitance level recorder. The low frequency peak in Fig. 4(c), which also appears in the pressure spectrum, is probably swell arriving by a rather tortuous path, from a storm which occurred in mid-Atlantic three days previous to the time of recording.

4.2 *Pressure and velocity power spectra*

The spectra of pressure and velocity show the same general features as the surface elevation though they are both modified by depth attenuation. A plot of the pressure and velocity spectra for PUV 15 is given in Fig. 5. The spectrum of the v component (parallel to the coastline) was generally much smaller than that for u. The peak of the v spectrum was usually less pronounced than that of u and p and it frequently occurred at a slightly higher frequency. This relative deficiency in the v spectrum at low frequencies probably results from the fact that the directional distribution is narrower in this part of the spectrum. Refraction also contributes to this effect since it tends to align the low frequency wave crests with the shore and hence reduce their v velocity component.

According to the linear theory the velocity and pressure spectra should be related according to

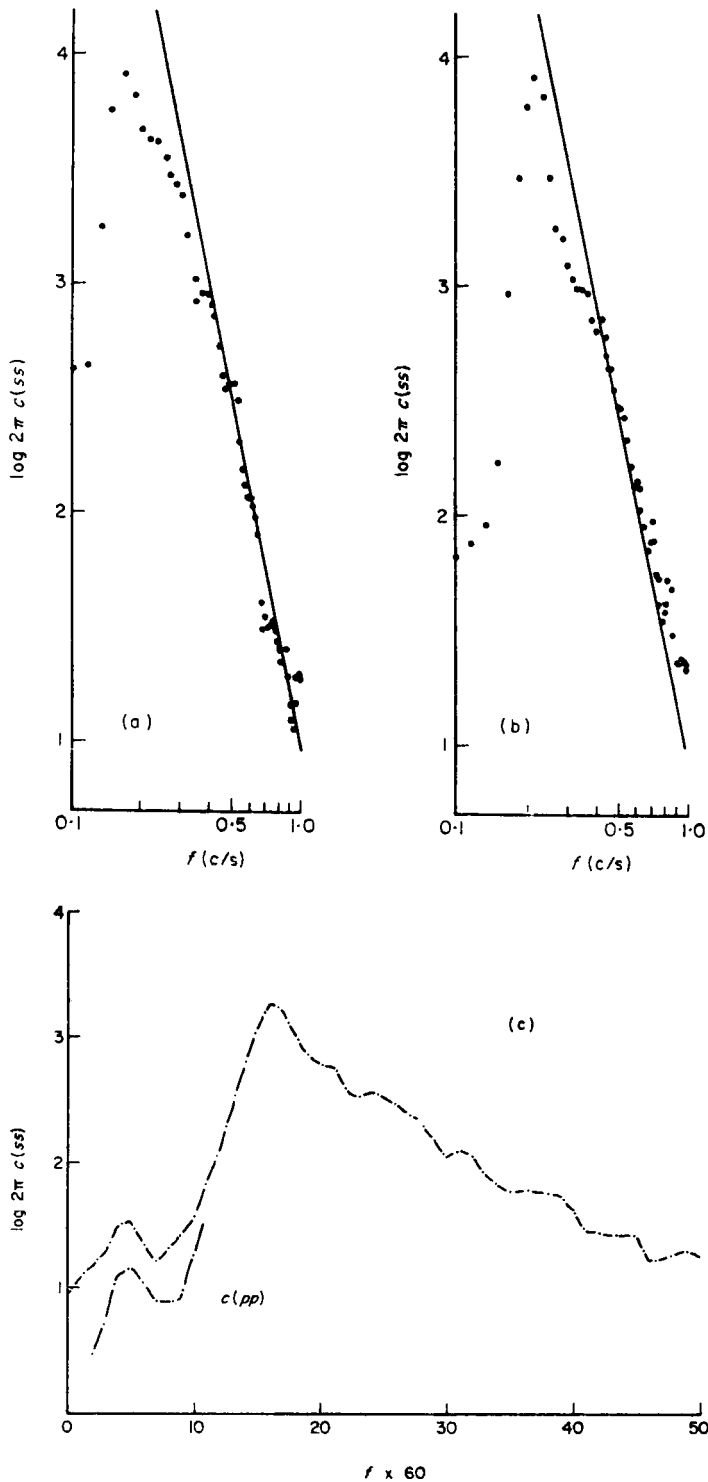$$\beta^2 = \frac{c(uu) + c(vv)}{c(pp)} = \left(\frac{gk}{\sigma}\right)^2 \qquad (4.1)$$

FIG. 4. (a) Surface power spectrum for SP 18; windspeed $=$ 20·5 knots, $\theta_w =$ 285°.
(b) Surface power spectrum for SP 6; windspeed $=$ 18·7 knots, $\theta_w =$ 255°.
(c) Surface power spectrum for SP 9; windspeed $=$ 15·3 knots, $\theta_w =$ 300°.
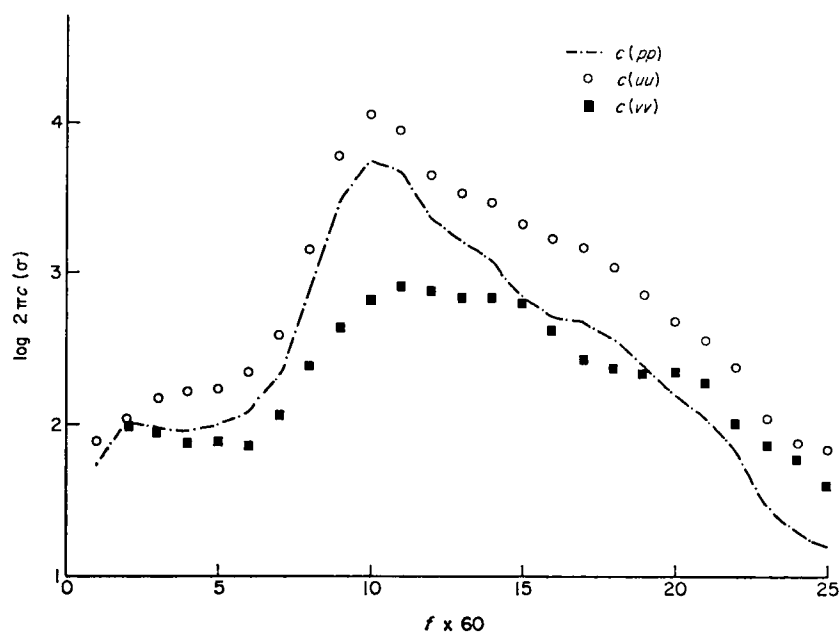$c(ss)$ in units of cm² s.

FIG. 5. Pressure and velocity power spectra for PUV 15; windspeed $= 19\cdot3$ knots, $\theta_w = 285°$; $h = 5\cdot03$ m. $c(pp)$ in units of cm^2 s. $c(uu)$ and $c(vv)$ in units of cm^2 s^{-1}.
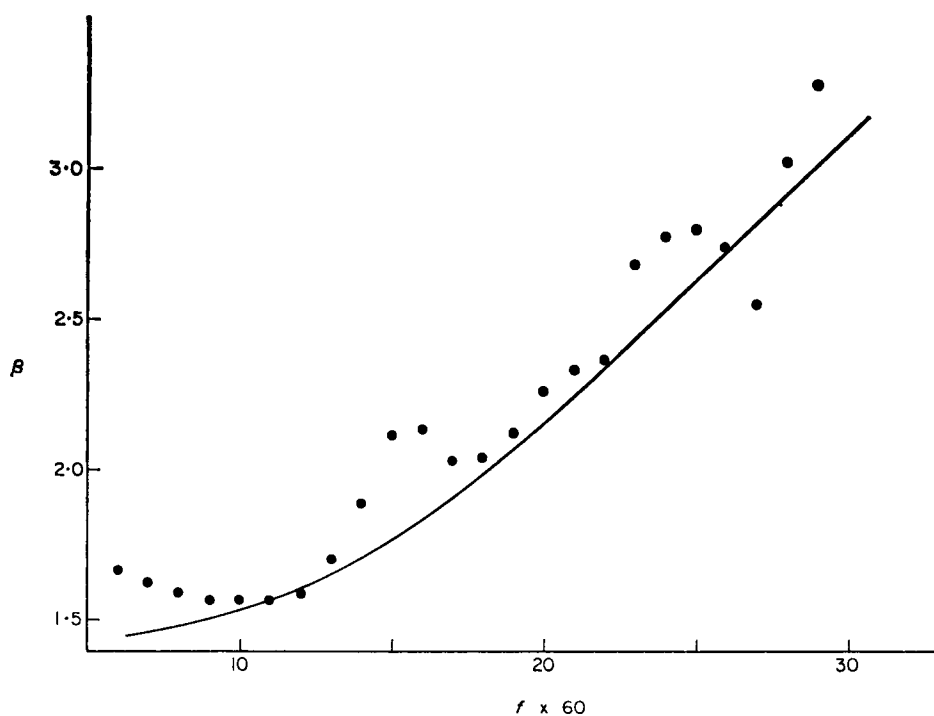

FIG. 6. The ratio β for PUV 15. The curve represents $\beta = \dfrac{gk}{\sigma}$.
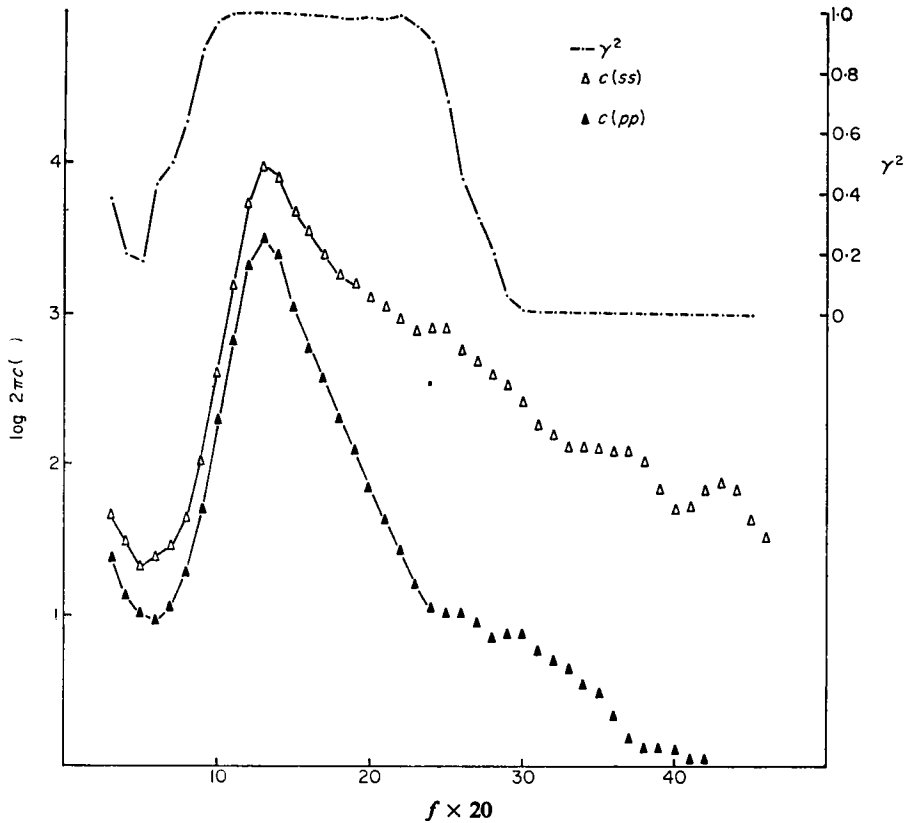
FIG. 7. Surface elevation and pressure spectra with γ^2 for SP 5 $h = 6 \cdot 00$ m.

The observed values of β are shown in Fig. 6 together with the curve representing $\beta = gk/\sigma$. There is satisfactory agreement between the two except for a certain amount of scatter in the observed points. This cannot be due to sampling errors since β is ratio of two quantities drawn from the same sample of a random process. Therefore, since the scatter corresponds to a noise level greater than that introduced by the instrumentation, we conclude that the variation in β results from a turbulent contribution to the spectra. Pressure and velocity fluctuations associated with turbulence are not subject to the relation (4.1) and may therefore account for the observed scatter.

Most of the points lie above the curve indicating that turbulence contributes mostly to the velocity spectra. This is what one might reasonably expect, since the pressure disturbance associated with turbulent velocity fluctuations is of the second order.

4.3 Attenuation with depth

The simultaneous surface and pressure spectra obtained from the SP records were used to determine the attenuation of the waves with depth. Where the coherency of the two parameters is close to unity, the attenuation factor may be computed from the ratio of the auto-spectra.

$$H_1' = \left(c(pp)/c(ss) \right)^{\frac{1}{2}}.$$

In all of the 20 records analysed, there was a frequency range around the spectral peak in which $\gamma^2 > 0 \cdot 9$. Fig. 7 represents the surface elevation and pressure spectra from a typical record together with their coherency. At high frequencies the coherency
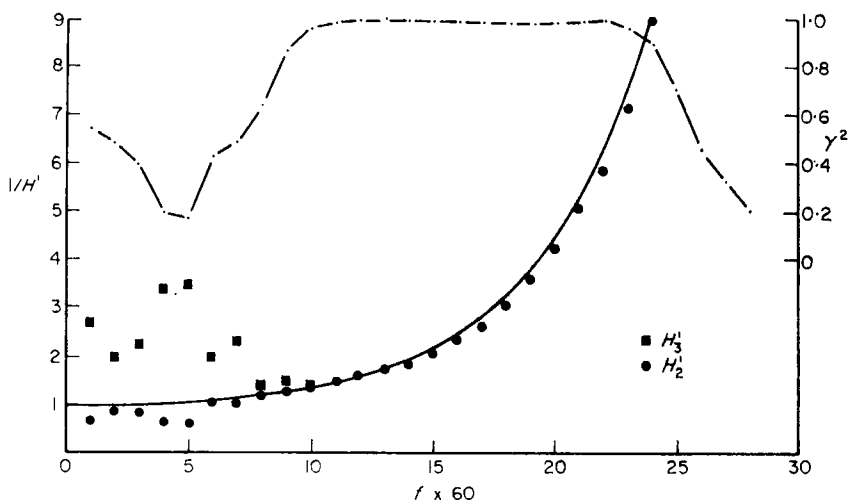
Fɪɢ. 8. Attenuation factor versus frequency for SP 5 $h = 6\cdot00$ m. $z = 3\cdot50$ m.

falls off due to severe attenuation of the pressure disturbance with consequent decrease in the signal to noise ratio. Assuming that all the noise at high frequencies is in the pressure record, a better estimate of the attenuation factor is

$$H_2' = c(sp)/c(ss).$$

Similarly if we assume that the noise is confined to the surface elevation record we have as the best estimate of H

$$H_3' = c(pp)/c(sp).$$

According to linear wave theory the attenuation is given by

$$H = \frac{\cosh k(z+h)}{\cosh kh}.$$

Values of $1/H'$ are compared with $1/H$ in Fig. 8. For the region where $\gamma^2 > 0\cdot9$ there is good agreement with the theory. Outside this range the variability of H' is clearly greater. At low frequencies both H_2' and H_3' have been plotted to indicate the extreme possible values of H'. It appears that even in this region the results are not inconsistent with classical theory.

Data from which $\gamma^2 > 0\cdot9$ from a number of records is shown in Fig. 9. The slight tendency for the ratio H'/H to be greater than unity at small values of H may be due to the effect of finite band-width in the analysis.

4.4 Comparison with previous results

Draper (1957) compared the spectra densities of surface elevation and bottom pressure in water of depth 6 m. Allowing for the large scatter, his results supported the classical law of attenuation at high frequencies but not for periods greater than 5 s. In this region of the spectrum, he concluded, rather surprisingly, that the waves were more severely attenuated than is indicated by first order theory. This result is supported at least qualitatively by Tsyplukhin (1963). Unfortunately, however, neither Draper nor Tsyplukhin have given details of the level of coherency in their measurements which, as can be seen from Fig. 8 plays a crucial role in determining the reliability of estimates of H. Certainly the present results do not
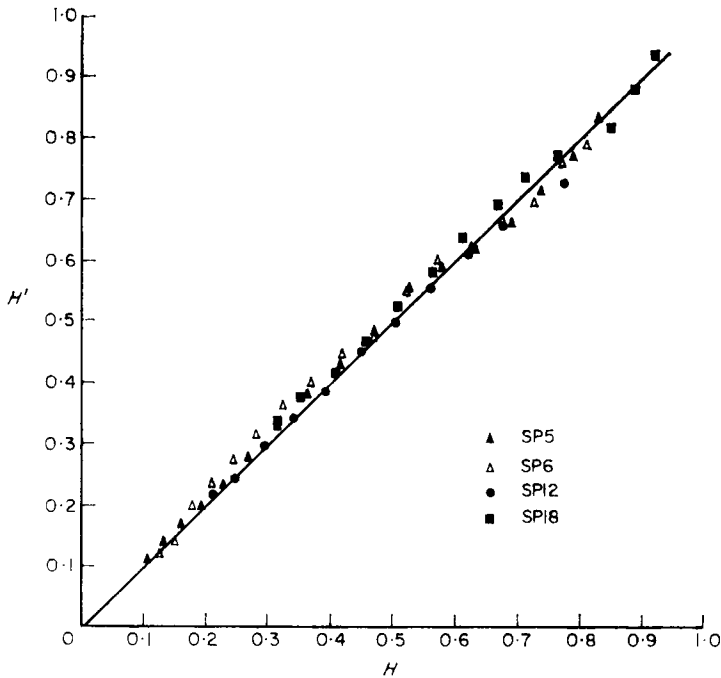
Fig. 9. Observed attenuation factor $1/H'$ vs $1/H$ from linear theory. $\gamma^2 > 0.9$
for all data.
SP 5; $h = 6.00$ m.
SP 6; $h = 5.54$ m.
SP 12; $h = 6.18$ m.
SP 18; $h = 5.61$ m.

support the idea of a departure from the classical law for periods less than 10 s.
It should however be noted that the spectral density at periods greater than 7 s was
very small compared with that at the peak of the spectrum. The spectra observed
by Draper and Tsyplukhin on the other hand both contained substantial energy at
low frequencies.

5. Directional properties of the waves

5.1 Selection of records and analysis

In this section we consider the directional characteristics of the wave spectrum
obtained from analysis of the PUV records. In all 40 such records representing
15 different sea states were anlaysed using the directional spectrum programme.
Of these, six groups were selected as suitable for more detailed study. The records in
each selected group were obtained at the same high water in synoptic situations in
which both wind speed and direction remained relatively constant over the relevant
fetch and duration, and the mean wind direction was between SW and NW. Within
this range of direction, the fetch is reasonably symmetrical about the mean wind
direction and corrections for the effects of refraction are more readily applied when
the incident angle is not too large.

The directional spectrum programme outputs the auto and cross-spectra of the
three time series, the angular harmonics of the modified directional spectrum and the
smoothed directional spectrum $F_3(\sigma, \theta)$. With the lag number $m = 40$ and $\Delta t = \frac{3}{4}$ s
the spectral estimates have a bandwidth of roughly $2\pi/30$ rad/s and stability cor-
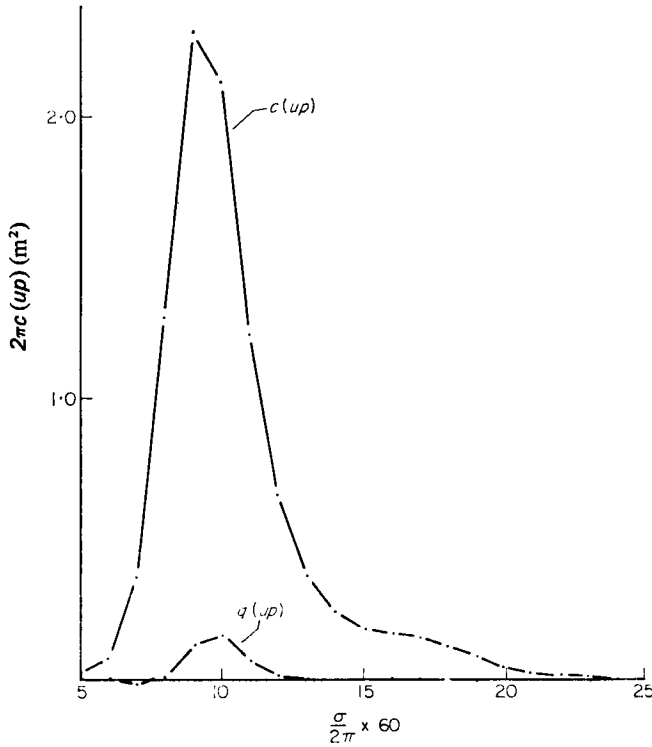responding to 40 degrees of freedom for a 10-min record.

J. H. Simpson

FIG. 10. Cross-spectra of the *u* velocity component and the pressure for PUV 7.

5.2 Cross-spectra of pressure and velocity

An example of the co- and quadrature spectrum of *u* and *p* is given in Fig. 10. The cospectrum is similar in form to the auto-spectra of *u* and *p* and like them exhibits a slight shoulder at approximately twice the dominant frequency. As expected the quadrature spectrum $q(up)$ of *u* and *p* is small in comparison with $c(up)$ throughout the spectrum.

The co- and quadrature spectra of each pair of components were used to deduce their relative phase $\Delta\phi$ and the coherency level of the two time series $\gamma^2(\sigma)$. Fig. 11 shows the phase of *u* and *p* versus frequency together with the corresponding plot of γ^2. There is some variation in the phase difference but its mean is clearly close to zero in agreement with the first order theory of progressive waves. The apparent undulation of $\Delta\phi$ along the frequency axis is probably due to the presence of a standing wave component resulting from partial reflection of the waves by the pier. The phase difference between pressure and velocity in a sinusoidal wave reflected by a vertical barrier may be shown to be just

$$\Delta\phi = \tan \Delta\phi = 2r \sin 2kL$$

where *r* the ratio of the reflected and incident amplitudes is small, and *L* is the distance of the detectors from the point of reflection. Since $|\Delta\phi| < 5°$ in the range of frequency where γ^2 is high, we may conclude that $r < 0.05$ indicating that only a very small fraction of the incident energy is reflected. The reflection in this case is from the array of piles supporting the pier so the variation of $\Delta\phi$ with wave number does not correspond to the theory for a single barrier.
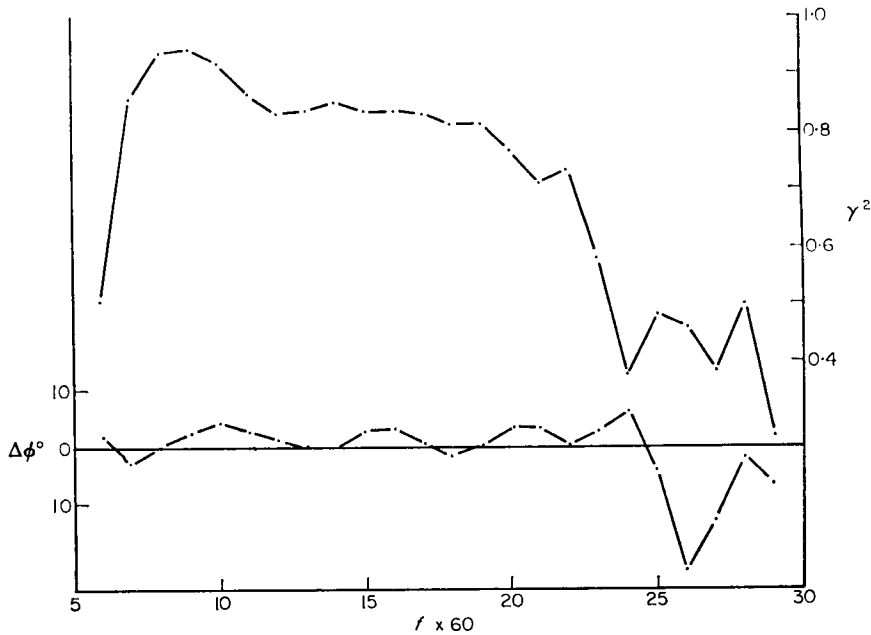
Fig. 11. Coherency γ^2 and relative phase $\nabla\phi$ for PUV 7.

When, as is the case given in Fig. 11, the mean direction of the waves is roughly parallel to u, the coherency γ^2 is a measure of the width of the directional spectrum since

$$
\gamma^2 = \frac{c^2(up)}{c(uu)\,c(pp)}\;\frac{\left(\int\limits_0^{2\pi} F\cos\theta\,d\theta\right)^2}{\int\limits_0^{2\pi} F\cos^2\theta\,d\theta \int\limits_0^{2\pi} F\,d\theta}.
$$

If $F(\sigma,\theta)$ simply consists of a delta function situated at $\theta=0$ we have $\gamma^2=1$ Otherwise γ^2 will be less than unity by an amount depending on the wdith of $F(\sigma,\theta)$.)

5.3 *Effects of refraction*

Since the bottom contours are regular and approximately parallel to the shore, the refraction of each wave component may be assumed to follow Snell's law

$$
\frac{\sin\theta_D}{\sin\theta_s} = \frac{k_s}{k_D}
$$

where θ_D and θ_s are the deep water and shallow water directions respectively referred to a line normal to the coast.

In assessing the effects of refraction on the directional spectrum we shall assume that each wave component in the spectrum is refracted independently. Strictly speaking this assumption is only justified when the wave amplitudes are sufficiently small, i.e. when

$$
a \ll \tfrac{4}{3} k^2 h^3.
$$

This condition was not usually satisfied in the present observations especially at the high frequency end of the spectrum where the waves had reached their limiting

steepness and were breaking. However, for the purpose of evaluating the deep water parameters of the spectrum, in the absence of a theory treating the non-linear aspects of refraction, we are forced to accept the assumption of linear refraction. At low frequencies where the spectrum is not saturated, this assumption is not too unreasonable, while at higher frequencies $k_s/k_D = 1$ so that the effects of refraction may be neglected.

It is shown in Longuet-Higgins (1956) that, for this linear case, the mean direction of each narrow frequency band in deep water is just

$$\bar{\theta}_D = \frac{k_s}{k_D} \bar{\theta}_s$$

where $\bar{\theta}_s$ is the observed mean value in shallow water and it has been assumed that the spectrum width ψ and $\bar{\theta}_s$ are both small. With these same assumptions, we also have

$$\psi_D = \frac{k_s}{k_D} \psi_s$$

for the deep water spectrum width.

Apart from changes in the directional properties of the waves, refraction may also affect their amplitude. The generalized form of the Burnside equation (Longuet-Higgins 1956) gives the amplification factor as

$$\frac{a_s}{a_D} = \left(\frac{dk_s}{dk_D} \frac{\cos \theta_D}{\cos \theta_s} \right)^{\frac{1}{2}}.$$

Assuming $h = 5\,\mathrm{m}$ for $f > 0\cdot1\,\mathrm{c/s}$ and $\theta_D < 40°$, we find numerically that $0\cdot85 < a_s/a_D < 1\cdot15$. Hence the effect on the spectrum should not be large providing we confine our interests to situations in which the major part of the wave energy is approaching the shore from the directions $|\theta_D| < 40°$.

5.4 *Mean direction of the waves*

A typical plot of the mean direction $\bar{\theta}$ vs frequency is given in Fig. 12. $\bar{\theta}$ is here referred to true north and is the direction from which the waves are approaching. If A_1 and B_1 are measured in shallow water then we may take

$$\bar{\theta}_D = \frac{k_s}{k_D} \bar{\theta}_s = \bar{\theta}_s \coth k_s h$$

as an estimate of the deep water direction providing the conditions for linear refraction are satisfied. The full curve in Fig. 12 represents the effect of refraction on waves approaching from the mean wind direction $\theta = 255°$.

In Table 1 the mean values of $\bar{\theta}_D$ for each of the selected groups of records are compared with the corresponding wind directions. The two are found to be in reasonable agreement.

Mean values of the skewness parameter m_3 are also given in the table. The variation of m_3 with frequency for a case in which the spectrum was nearly symmetrical is given in Fig. 12. Non-zero skewness may arise either from asymmetry of the fetch or refraction at large angles of incidence, or from non-uniformity of wind speed and direction over the generating area. In view of the selection already made, the latter possibility seems the most likely cause of the marked skewness found in a number of selected groups. A general tendency to negative skewness however, which is evident in the data, probably results from the fact that fetches

from the SW and S were generally longer than those from the NW and N. In any case it is only groups with low skewness which are suitable for comparison with theory.
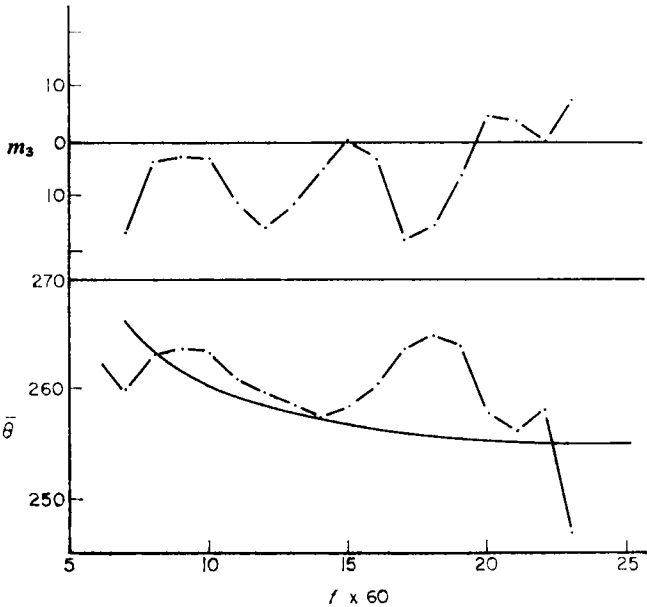

FIG. 12. Deep water direction θ and skewness m_3 for PUV 8. The curve represents the effect of linear refraction on waves approaching from the mean wind direction $\theta_w = 255°$.

Table 1

Group	Record Nos	Wind speed W	Wind direction θ_w	θ_D	m_3 (deg)	Fetch (km)
3	8	26·8	255	258	− 3·4	210
	9			262	− 4·6	
4	15	19·3	285	267	− 5·2	220
	16			269	− 4·6	
6	19	18·7	255	249	−37·2	210
	20			247	−39·9	
7	23	15·3	300	299	+ 6·9	98
	24			298	+ 0·6	
8	26	26·8	250	243	−33·2	210
	27		249		−21·2	
10	34	20·5	285	259	−20·6	190

W = mean of previous six hours at Blackpool.
θ_w = mean of previous six hours at Blackpool.
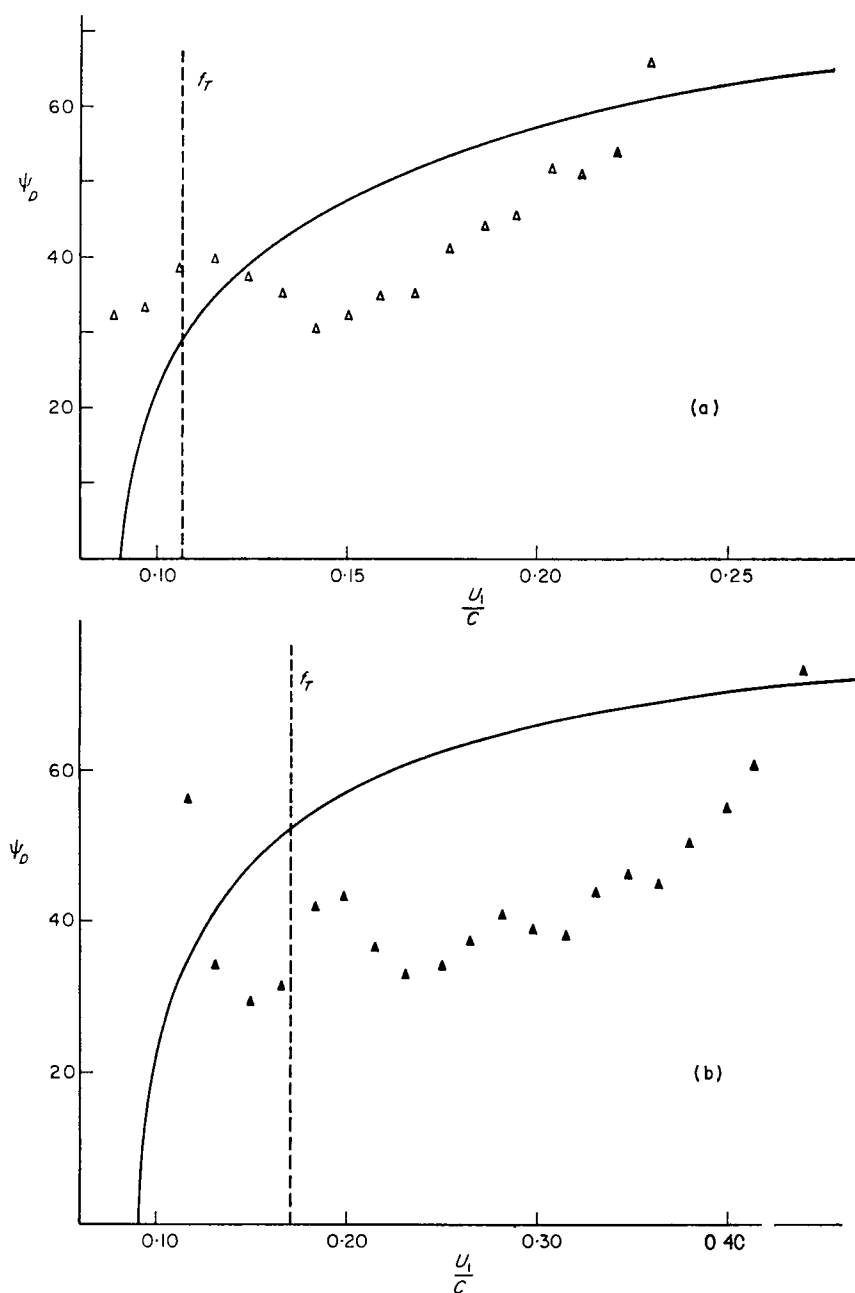$\bar{\theta}$ and $\bar{m}_3$ are mean values for the dominant region of spectrum.

FIG. 13. Deep water spectrum width ψ_D. (a) Mean ψ_D for PUV 15 and PUV 16; windspeed 19·3 knots; fetch = 220 km. (b) Mean ψ_D for PUV 7 and PUV 8; windspeed 29·1 knots; fetch = 210 km. The curve represents the resonance angle given by Phillips theory. The broken line indicates the transition frequency.

Table 2

Hourly mean wind data for 1965 May 12 and 13

Time	Blackpool		Ronaldsway		Valley	
	Speed	Direction	Speed	Direction	Speed	Direction
2200/12/4	15	270	18	280	15	280
2300	14	280	20	290	14	270
0000/13/4	15	270	22	280	15	270
0100	16	280	19	280	16	260
0200	12	290	22	280	16	260
0300	15	280	18	270	18	260
0400	18	280	17	270	19	270
0500	19	280	19	280	20	260
0600	20	280	20	280	20	270
0700	19	290	20	280	20	270
0800	20	290	20	280	19	270
0900	19	290	23	280	20	270

Mean speed for 10 h (last 5 h double weighted) = 19·3 knots.
Mean direction for 10 h (last 5 h double weighted) = 278°.

5.4 *Spectrum width parameters*

Fig. 13(a) shows ψ_D for the group 4 data which was obtained after a period of unusually consistent wind conditions (see Table 2). The values of ψ_D are plotted against the dimensionless parameter u_1/c where u_1 is a parameter of the logarithmic distribution.

$$u = u_1 \log_e z/z_0.$$

The curve represents the resonance angle predicted by Phillips' theory.

$$\psi = \sec^{-1}\left(\frac{u_1}{c}\log\frac{2\pi}{\Omega} - 2\log\frac{u_1}{c}\right)$$

$$\Omega = \frac{g z_0}{u_1{}^2}.$$

The value of Ω is not known precisely but varying Ω by a factor of five about an approximate value of $1\cdot3 \times 10^{-2}$ does not seriously modify the resonance angle (see Longuet-Higgins, Cartwright & Smith (1963)). The dashed line in Fig. 13(a) indicates the transition frequency defined by Phillips & Katz (1961). For small values of u_1/c, ψ_D is not inconsistent with the resonance angle but in the range $0\cdot14 < u_1/c < 0\cdot22$ the observed width is appreciably smaller than indicated by the theory. This narrowing of the spectrum occurs at a value of u_1/c just above that required, according to the theory, for the transition to exponential growth at this fetch. There is a similar reduction in the width relative to the resonance angle in the group 3 data given in Fig. 13(b) and in this case the observed points lie below the curve over a wider range of u_1/c. However, it seems probable that the generally narrower spectra observed in this case, resulted from the fact that the wind speed over the generating area had fallen to 26 knots at the time of recording from a peak of 33 knots six hours previously.

These results for ψ_D are in substantial agreement with those found in open sea conditions by Longuet-Higgins, Cartwright & Smith (1963) using the pitch and roll buoy. In so far as ψ_D appears to correspond to the resonance angle in that region of the spectrum where the resonance mechanism alone should be responsible
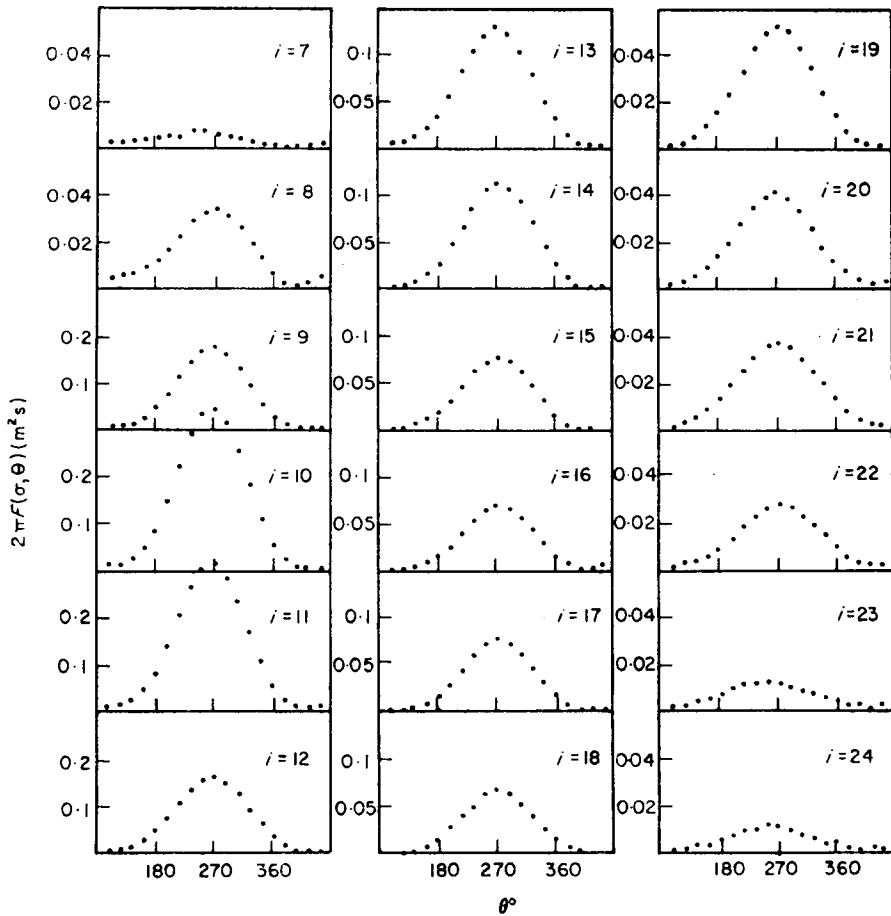
FIG. 14. Smoothed directional spectrum F_3 (σ, θ) for PUV 15; windspeed 19·3 knots; $\theta_w = 285°$. $\sigma = 2\pi i/60$.

for growth, the results lend support to the Miles-Phillips theory. The relative narrowing of the spectra at higher values of u_1/c is consistent with the shear flow instability mechanism. However recent work by Snyder & Cox (1966) and Barnett & Wilkerson (1967) indicates that wave growth by an instability mechanism is an order of magnitude stronger than predicted by Miles. Whatever the nature of the instability, it seems probable that a transition in the growth regime is responsible for the observed spectrum width falling to a minimum considerably less than the resonance angle.

At large values of u_1/c the spectrum appears to be rather broad but the amount of reliable data in this range is limited on account of the poor signal to noise ratio at high frequencies and the absence of data for wind speeds greater than 30 knots.

5.5 Smoothed estimates of the directional spectrum

From the first five angular harmonics of the modified directional spectrum we have as a smoothed estimate of the surface spectrum

$$F_3(\sigma, \theta) = \frac{1}{H^2(\sigma)} \left(\tfrac{1}{2}A_0 + \tfrac{2}{3} (A_1 \cos\theta + B_1 \sin\theta) + \tfrac{1}{6} (A_2 \cos 2\theta + B_2 \sin 2\theta) \right)$$
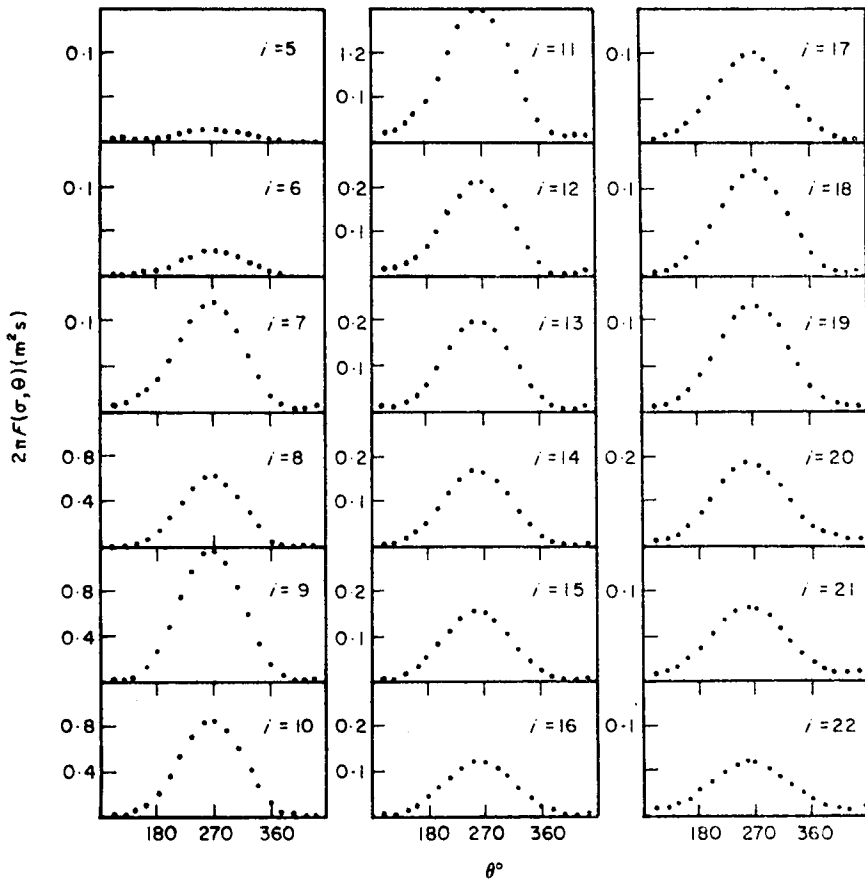
where $H(\sigma)$ is the attenuation function.

FIG. 15. Smoothed directional spectrum F_3 (σ, θ) for PUV 8; windspeed 29·1 knots; $\theta_w = 255°$. $\sigma = 2\pi i/60$.

$F_3(\sigma, \theta)$ for groups 3 and 4 are given in Figs 14 and 15. In all these spectra the modal direction varies little with frequency. The directional distribution is roughly symmetrical at all frequencies and it is in every case unimodal. It should be remembered however, that on account of the considerable width of the filter function, the apparent directional distribution is very broad so that any bimodality in the true spectrum would probably be obscured.

5.6 Comparison with SWOP spectrum

The directional spectra group 4 (PUV 15 and 16) deserve particular attention since the wind field was particularly steady during the previous twelve hours. Table 2 shows the hourly wind data for this period. The direction at all three stations was never more than 10° from the mean throughout the period. The wind speed was more variable but was very consistent, if one considers only the wind experienced by waves crossing the Irish Sea at the group velocity corresponding to the spectrum peak ($T = 6$ s). The mean velocity and direction found from a weighted average of the data in italics in Table 2 is wind speed 19·3 knots, direction 278°.

It is interesting to compare the power spectra for this case with those found in oceanic conditions in the SWOP experiment when the wind speed was almost identical (18·7 knots). The surface power spectra are shown in Fig. 16. The SWOP spectrum extends to much lower frequencies and has a greater energy content, the variance
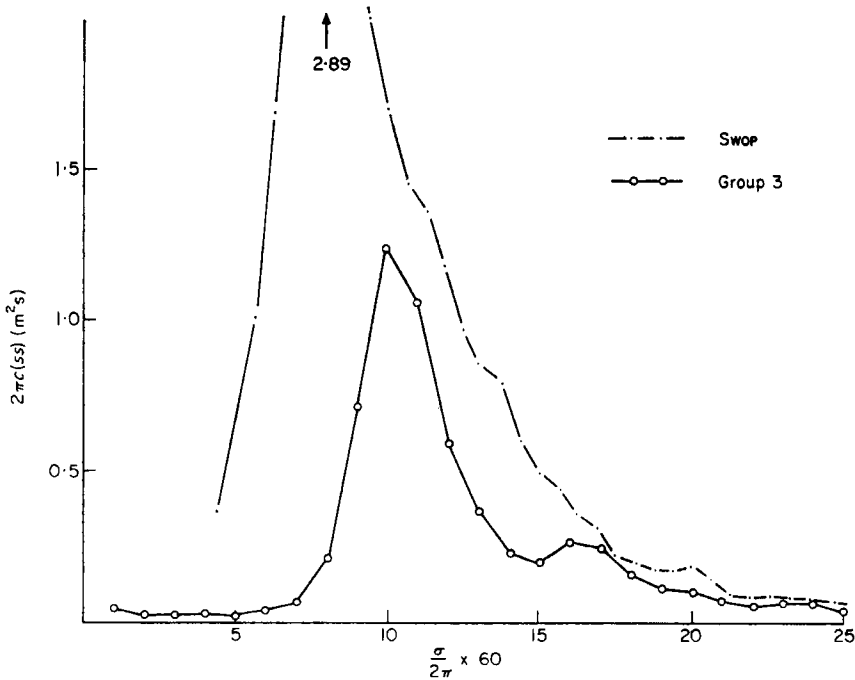
FIG. 16. Surface power spectrum for group 4 and SWOP spectrum. For group 4 spectrum: windspeed = 19·3 knots at 10 m overland; degrees of freedom $k = 40$. For SWOP spectrum: windspeed = 18·7 knots at 15–18 ft over the sea; degrees of freedom $k \geqslant 174$ except at low frequencies where $k = 20$.

being about three times that of the group 4 spectrum. The fetch in the case of SWOP was less than the 200 km in the Irish Sea so the difference in the spectra must be due to other factors.

The most likely cause of this marked difference between the spectra is the effect of the bottom which, apart from modifying the deep water amplitude, also caused frictional dissipation of the waves. It is readily shown that the rate at which energy is lost per unit area by waves of amplitude a in water of depth h is given by

$$D = \kappa \rho a^3 \, F(h, \sigma); \quad F(h, \sigma) = \tfrac{4}{3} \sigma^3 \, \mathrm{cosech}^3 \, kh$$

where κ is the frictional constant.

Putnam & Johnson (1949) have used this formula with $\kappa = 0\cdot01$ to evaluate the effect on waves of height 5 ft moving up a beach of slope 1 : 300. Before they reach a depth of 5 m, the waves experience an energy loss of ~ 12 per cent due to friction. In addition to this there is a reduction in energy density due to the presence of the bottom, the combined loss being ~ 25 per cent. At Blackpool the mean bottom slope out to the 20 m contour is of order 1 : 300 but increases to about 1 : 100 near the shore. Hence the above figure should represent an upper limit to the loss in this case, and could account for the difference between the spectra at frequencies above the peak of the group 4 spectrum. Losses on entering shallow water cannot however be responsible for the low level of the group 4 spectrum in the vicinity of the SWOP spectrum peak.

It seems plausible that the growth of the low frequency components is inhibited by the effects of bottom friction in the generating area (mean depth ~ 50 m). An equilibrium may be established in which the energy input to the low frequencies is just balanced by the frictional dissipation. The rate of the energy input to a given

frequency band can be roughly estimated on the assumption that in the initial stage of development the energy increase is linear in time (as indicated by the resonance model). When this is done it is found that the dissipation by bottom friction with $\kappa = 0.01$ will not balance the input unless the wave amplitude is rather large. Increasing κ by an order of magnitude would still not adequately inhibit development of low frequencies. One must conclude therefore that the initial rate of growth of the low frequencies is less than estimated from the assumption of the linear growth, or that the frictional mechanism must be augmented in some way, possibly by interaction of the waves with tidal streams.

In a recent paper Hasselmann & Collins (1968) have computed the dissipation due to bottom friction for a broad frequency spectrum in the presence of a mean current. The results indicate that dissipation may be greatly increased by the presence of a current of the order of the tidal streams in the Irish Sea.

Darbyshire's (1961) coastal spectrum formula gives the period as 6·5 s in reasonable agreement with observations but the predicted variance is too high (1910 cm^2 compared with the observed value of 1060 cm^2). This difference here may be due, in part at least, to the fact that Darbyshire's spectrum is based on observations made in deeper water from the Morecambe Bay lightship, where the influence of bottom friction should be smaller.

The spectrum width was also compared with the results obtained by SWOP. Since the stereo method gives only the even harmonics of the spectrum, we use the width Γ based on the second harmonic i.e.

$$\Gamma = \frac{A_0 - C_2}{A_0 + C_2}; \quad C_2{}^2 = A_2{}^2 + B_2{}^2.$$

The spectrum proposed by the authors of SWOP as the best fit to the results gives Γ as

$$\Gamma^2 = \frac{0.75 - 0.41 R(\sigma)}{1.25 + 0.41 R(\sigma)}; \quad R(\sigma) = e^{-\frac{1}{2}(\sigma V/g)^4}$$

where V is the windspeed at anemometer height.

Fig. 17 shows the observed values of Γ corrected for refraction against the parameter $\sigma V/g$ together with the corresponding values of ψ_D (in radians) and the curve representing the SWOP results. The observed values of Γ agree well with those of ψ_D. They do not however, support the form of the empirical spectrum. In particular the marked minimum in the observed width is not reflected in the SWOP spectrum.

5.6 Results of array measurements

The derivative records were analysed by means of an extended version of the directional spectrum programme using the theory given above. The results indicated that the signal to noise ratio of the velocity derivatives was generally lower than had been anticipated. Fig. 18 shows a plot of the ratio δ and the curve representing α^2/k^2. The observed values all lie well above the curve indicating a high noise level over the entire spectrum.

The poor signal/noise ratio means that estimates of the higher angular harmonics were rather variable and often contravened the inequality.

$$A_n{}^2 + B_n{}^2 \leqslant A_0{}^2.$$

The results were found to be most unreliable in heavy seas. With smaller wave heights the signal/noise ratio was appreciably better and a number of satisfactory
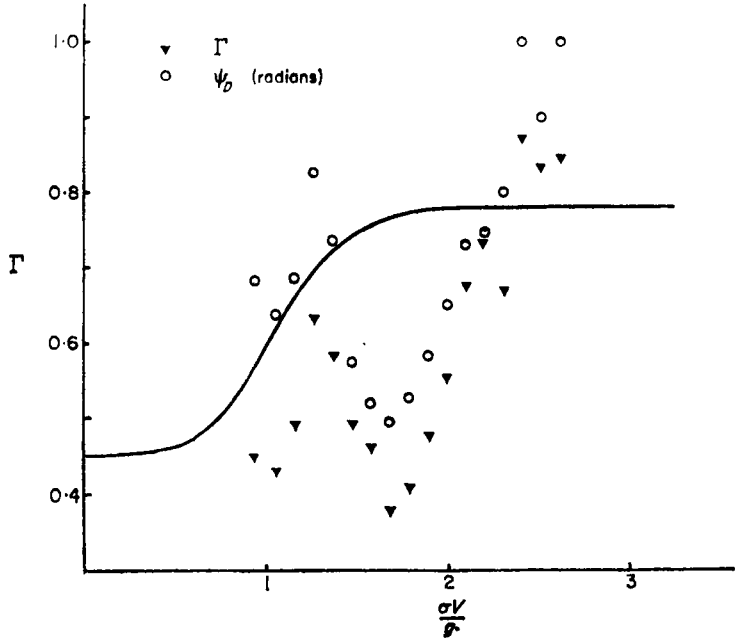
Fig. 17. Spectrum width parameters Γ and ψ_D for PUV 15. The curve represents Γ as given by the SWOP spectrum.
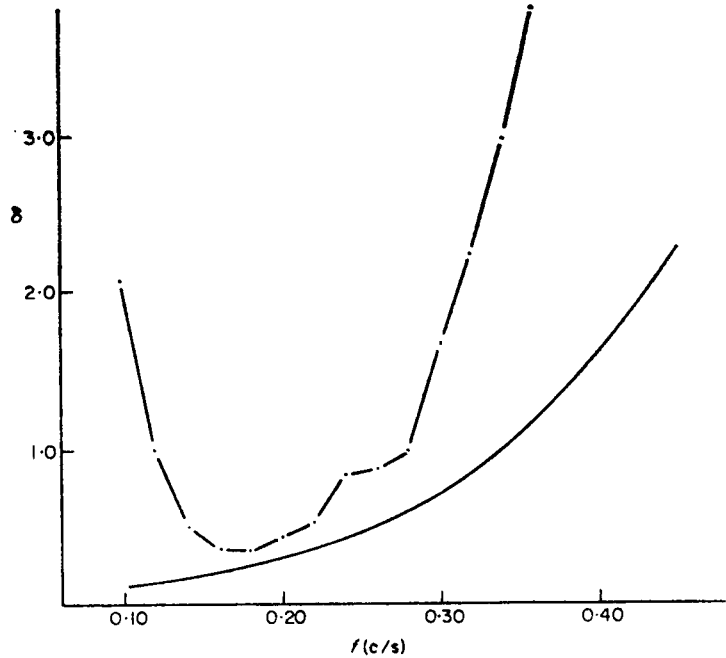

Fig. 18. The ratio δ for derivative record 24. The curve represents $\delta = \dfrac{gk^2}{\sigma}$.
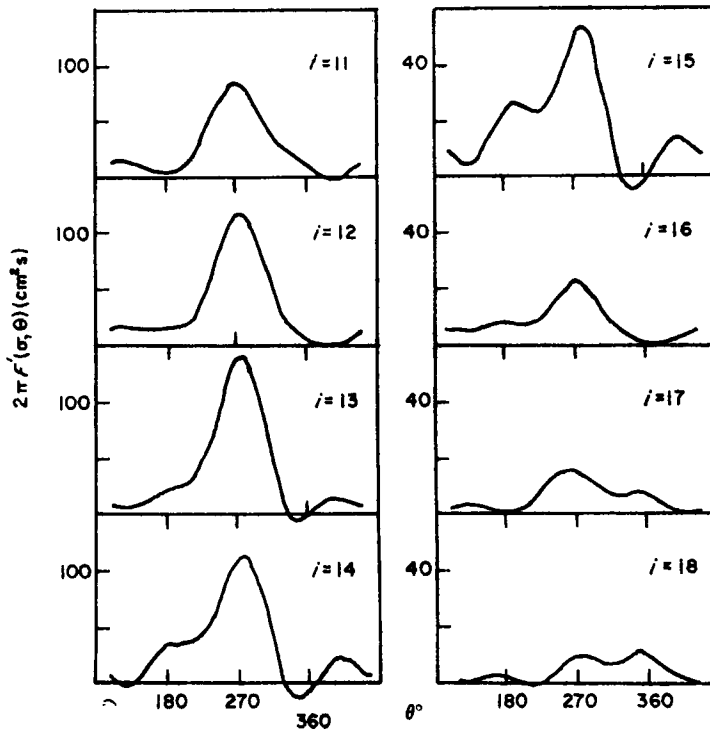
FIG. 19. Smoothed directional spectrum estimate F_4 (σ, θ) for derivative record 20.
$h = 6\cdot02$ m. $\sigma = 2\pi i/60$.

estimates of the angular harmonics were obtained under such conditions. The estimate F_4' of the modified directional spectrum for the least noisy part of the spectrum is shown in Fig. 19.

The results are apparently reasonable except for small negative values which occur at some frequencies. The local wind at the time of recording was light (7 knots NNW), but its effect can be seen in the small peak in the directional spectrum in the two highest frequency bands shown. The remainder of the energy is mainly swell from a direction slightly north of west.

The fact that the results obtained in rough seas were not satisfactory must be attributed to the turbulent velocity fluctuations induced by the pier structure. For practical reasons the array was necessarily rather close to the pier, and turbulent eddies generated by the pier supports were undoubtedly influencing the flow in the vicinity of the array.

In the case of smaller waves, the excursions of the individual water particles were smaller so the influence of the pier was appreciably less.

The behaviour of the high frequency part of the spectrum also indicated the presence of a high degree of turbulence in heavy seas. As explained above, the derivative spectra should fall to zero at high frequencies. This only happened in relatively light seas. When the waves were larger the spectra of all the derivatives remained at an appreciable level even at the high frequency limit.

Acknowledgments

I am indebted to Professor K. F. Bowden for many helpful suggestions and comments during the course of this study. I would also like to thank the technical

staff of the Liverpool University Department of Oceanography for their help in the construction and maintenance of the recording apparatus, and the management of the South Pier at Blackpool for providing an excellent site for the observations.

Marine Science Laboratories,
Menai Bridge,
Anglesey.

1968 *May.*

References

Barnett, T. P. & Wilkerson, J. C., 1967. *J. mar. Res.*, **25**, No. 3.

Blackman, R. S. & Tukey, J. W., 1958. *The measurement of Power Spectra*, Dover, New York, 190 pp.

Bowden, K. F. & Fairbairn, L. A., 1952. *Phil. Trans. R. Soc.*, **A244**, 224–335.

Bowden, K. F. & White, R., 1966. *Geophys. J. R. astr. Soc.*, **12**, 33–54.

Burling, R. W., 1955. Wind generation of waves on water, Ph.D. Thesis, University of London.

Cartwright, D. E., 1961. The use of the directional spectra in studying the output of a wave recorder on a moving ship, in *Ocean Wave Spectra*, Prentice Hall, New Jersey.

Cartwright, D. E., 1962. *The Sea*, Vol. 1, pp. 567–589, Wiley, New York.

Cartwright, D. E. & Smith, N. D., 1964. Buoy techniques for obtaining directional wave spectra, in *Buoy Technology*, Marine Technology Society, Washington.

Cote, L. J. *et al.*, 1957. The directional spectrum of a wind generated sea as determined from data obtained by the Stereo Wave, Observation Project, New York University.

Darbyshire, J., 1961. The one-dimensional wave spectrum in the Atlantic Ocean and in coastal waters, in *Ocean Wave Spectra*, Prentice Hall, New Jersey.

Draper, L., 1957. *Houille blanche*, **12**, 926–31.

Harris, M. J. & Tucker, M. J., 1963. *Instrum. Pract.*, **17**, 1055–1059.

Howe, M. R., 1960. Measurements of the structure of turbulence in a tidal current, Ph.D. Thesis, University of Liverpool.

Lamb, H., 1932. *Hydrodynamics*, 6th edn, Dover, New York.

Hasselmann, K. & Collins, J. I., 1968. *J. mar. Res.*, to be published.

Longuet-Higgins, M. S., 1946. The measurement of water velocity by electromagnetic induction, Admiralty Research Laboratory Report 102.22/31/M.

Longuet-Higgins, M. S., 1956. *J. fluid Mech.*, **1**, 163–176.

Longuet-Higgins, M. S., Cartwright, D. E. & Smith, N. D., 1961. Observations of the directional spectrum of sea waves using the motions of a floating buoy, in *Ocean Wave Spectra*, Prentice Hall, New Jersey.

Miles, J. W., 1957. *J. fluid Mech.*, **3**, 185–204.

Miles, J. W., 1960. *J. fluid Mech.*, **7**, 469–478.

Miles, J. W., 1967. *J. fluid Mech.*, **30**, 163–175.

Phillips, O. M., 1957. *J. fluid Mech.*, **4**, 417–445.

Phillips, O. M., 1958. *J. fluid Mech.*, **4**, 426–434.

Phillips, O. M. & Katz, E. J., 1961. *J. mar. Res.*, **19**, 57–69.

Phillips, O. M., 1966. *The Dynamics of the Upper Ocean*, Cambridge University Press.

Putnam, J. A. & Johnson, J. W., 1949. *Trans. Am. geophys. Un.*, **30**, 67–74.

Tsyplukhin, V. F., 1963. *Okeanologiya*, **3**, No. 5.

Snyder, R. L. & Cox, C. S., 1966. *J. mar. Res.*, **24**, No. 2.

Tucker, H. J. & Charnock, H., 1954. *Coastal Engng*, **5**, 176–188.